Published in final edited form as:

Kidney Int. 2021 November ; 100(5): 1001–1011. doi:10.1016/j.kint.2021.04.032.

Basic Principles and New Advances in Kidney Imaging

Anna Caroli[1], **Andrea Remuzzi**[2], **Lilach O. Lerman**[3]

[1.]Bioengineering Department, Istituto di Ricerche Farmacologiche Mario Negri IRCCS, Bergamo, Italy

[2.]Department of Management, Information and Production Engineering, University of Bergamo, Dalmine (BG), Italy

[3.]Division of Nephrology and Hypertension, Mayo Clinic, Rochester, MN, USA

Abstract

Over the past few years, clinical renal imaging has seen great advances, allowing assessments of kidney structure and morphology, perfusion, function and metabolism, oxygenation, as well as microstructure and interstitium. Medical imaging is becoming increasingly important in the evaluation of kidney physiology and pathophysiology, showing promise in management of patients with renal disease, in particular with regard to diagnosis, classification, and prediction of disease development and progression, monitoring response to therapy, detection of drug toxicity, and patient selection for clinical trials.

A variety of imaging modalities, ranging from routine to advanced tools, are currently available to probe the kidney both spatially and temporally, particularly ultrasonography, computed tomography, positron emission tomography, renal scintigraphy, and multiparametric magnetic resonance imaging. Since the range is broad and varied, kidney imaging techniques should be chosen based on the clinical question and specific underlying pathological mechanism, considering contraindications and possible adverse effects. Integration of different modalities providing complementary information will likely bestow the greatest insight into renal pathophysiology.

This review aims to highlight major recent advances in key tools currently available or potentially relevant for clinical kidney imaging, with a focus on non-oncological applications. The review also outlines the context of use, limitations, and advantages of different techniques, and finally emphasizes gaps for future development and clinical adoption.

Corresponding author: Anna Caroli, PhD, Bioengineering Department, Istituto di Ricerche Farmacologiche Mario Negri IRCCS, Via Camozzi 3, 24020 Ranica (BG), Italy, Tel. +39-035-4535381, Fax. +39-035-4535371, acaroli@marionegri.it.

Editor’s note:
As part of Kidney International’s series on new visualizing techniques, Drs. Caroli, Remuzzi and Lerman discuss advances in clinical imaging focusing on new ways of using standard technology ranging from ultrasound to positron emission tomography.

Disclosures
Dr. Lerman is an advisor to AstraZeneca and Janssen Pharmaceuticals. The authors declare no conflicts of interest.

Keywords

renal biopsy; kidney development; chronic kidney disease

Introduction

Despite the complexity and heterogeneity of renal structure and function, clinical management of kidney diseases is mainly based on relatively crude laboratory tests. To obtain greater understanding of disease mechanisms and stages, high-resolution imaging techniques have been developed to probe the kidney both spatially and temporally. These tools have subsequently evolved into an essential part of evaluation of kidney physiology and pathophysiology. The advent of tomographic imaging has been particularly pivotal, enabling noninvasive high-resolution discrimination of intra-renal compartments (including cortex, medulla, and collecting system) rapidly enough to monitor functional processes, and with versatility that leverages and matches the rapidly growing understanding of pathophysiological mechanisms.

Several fundamental tools are used in clinical kidney imaging. Given its low cost and availability, despite limited resolution and operator-dependence, conventional ultrasonography has become a routine tool in renal disease. Contrast-enhanced (CE) ultrasound (CEUS), using inert gas microbubbles as contrast agents to investigate microvascular perfusion with reasonably good spatial resolution[1], and ultrasound elastography (UE), enabling in-vivo evaluation of mechanical properties of soft tissue, have introduced novel applications based on ultrasound wave propagation[2,3].

Over the past decade, magnetic resonance imaging (MRI) has emerged as a promising technique for characterization of evolving renal pathophysiology[4]. Structural and functional MRI can be performed in a single multiparametric session, enabling investigation of kidney structure, microstructure, and functional heterogeneity. With notable versatility and no need for contrast agents or ionizing radiation, it is well-suited to serial applications, even in patients with impaired renal function. Its limitations include cost, prolonged scanning, and several clinical contraindications, like metal implants or devices.

Renal scintigraphy is a nuclear medicine technique using radiolabelling to provide combined functional and anatomical information. Depending on the radiopharmaceutical used, it allows both static and dynamic imaging of the kidney. Its limitations include limited spatial resolution, long acquisition time, a high radiation dose and image quality dependence on several factors.[5] X-ray computed-tomography (CT) offers fast scanning and high spatial and temporal resolution, yet involves ionizing radiation exposure and often requires using iodinated and potentially nephrotoxic contrast material. Positron emission tomography (PET) has low spatial resolution (3–5 mm), uses radiotracers, and is costly and time-consuming, but provides unique metabolic information regarding tissue uptake.

Therefore, appropriate selection of imaging tools can be of enormous value in evaluating the kidney. Using well-defined physiological challenges or molecular targeting further enhances their specificity and sensitivity. Hence, imaging plays a key role in management of patients with renal disease. Medical imaging currently guides a broad range of clinical applications, including diagnosis, classification, and prediction of disease development and progression, monitoring response to therapy, detection of drug toxicity, and patient selection for clinical trials.

This review aims to provide an overview of imaging techniques currently available to probe the kidney (focusing on non-oncological applications), highlight new advances, and emphasize gaps for further development.

Renal structure and morphology

Several imaging-derived aspects of renal anatomy are potentially useful for management of patients with kidney disease.

Renal size.

Changes in kidney dimensions reflect functional deterioration and disease progression. Renal length or volume are useful in evaluation of kidney transplant recipients, and patients with aging, renovascular, or urinary tract diseases, and is central in evaluating progression of polycystic kidney disease (PKD)[6]. Assessment of intra-renal regions might also be revealing; for example, smaller medullary volume in healthy donors predicts subsequent graft failure[7]. Generally, 3D methods like CT and MRI reflect renal dimensions more faithfully than 2D methods like ultrasonography (Figure 1), without relying on geometric assumptions.

Renal roughness.

An irregular cortical surface may indicate nephrosclerosis. CE-CT detects roughness of the kidney exterior in older vs. younger kidneys, independent of cortical atrophy, providing a quantitative index of nephrosclerosis *in-vivo*[8]. However, studies are needed to determine its sensitivity, as this phenotype is likely limited to advanced renal damage.

Adiposity.

Deposition of perirenal adipose tissue is associated with adverse renal and cardiovascular events. Perirenal fat is measurable using CT[9], MRI, or ultrasound . MRI-quantified renal sinus fat increases with glucose intolerance, possibly linking metabolic disease and chronic kidney disease (CKD)[10]. Moreover, B-mode ultrasound-derived perirenal fat negatively correlates with estimated glomerular filtration rate (GFR) in diabetic patients[11].

Kidney stones.

In patients with nephrolithiasis, stone size, composition, and location are important for clinical decision-making. CT is considered the most accurate for initial diagnosis, because ultrasonography might miss small stones.[12] Exciting developments in dual-energy and photon-counting detector CT[13] allow identification of urate and calcium stones, and possibly rarer stone types[14]. Developments to increase resolution and decrease radiation exposure are needed to support non-CE-CT as a first-line tool for evaluation of these patients.

Angiography/Urography.

Traditionally performed by 2D X-ray imaging, evaluation of the renal artery and ureter to detect renal vascular or urinary tract issues and for preoperative evaluation of kidney donors can now be effectively achieved by CT and MRI[15]. Paramagnetic iron-oxide nanoparticles, like Ferumoxytol, may provide a safer alternative to gadolinium in MR angiography[16]. MR urography, illustrating the urinary tract structure and function, is a promising alternative to intravenous urography, especially in the paediatric population[17]. Non-CE MRI offers important advantages over CE-CT for renal artery evaluation[18], including elimination of risk and cost associated with contrast administration and suitability for repeated acquisition, yet must be weighed against potential overestimation of the degree of stenosis and relatively long acquisition times.

Renal Perfusion

Cortical, medullary, and total renal blood flow (RBF) and perfusion (RBF/unit tissue) are influenced by renal function, yet their independent regulation encourages direct measurement of renal hemodynamics. In human subjects, para-aminohippurate (PAH) clearance is useful, but provides no information on individual kidneys or their compartments, underestimates RBF, and is affected by glucosuria[19]. Scintigraphy, CT, MRI, and PET overcome many such limitations. A well-established method to assess split renal function and outflow conditions is dynamic renal scintigraphy. Both 99mTc-DTPA and 99mTc-MAG3 can assess relative renal allograft perfusion after transplantation[20]. 99mTc-PAH, owing to its fast kinetics, excretion properties, and high-quality images, shows promise as a substitute for 99mTc-DTPA[21], and 99mTc-EC scintigraphy for diagnosis of obstructive uro-nephropathy[22]. Multi-detector CE-CT affords quantifications of total and regional perfusion using indicator-dilution curves in patients with renovascular disease and hypertension[23,24], and GFR can be concurrently quantified as well[25].

PET, a reference standard for quantitative cortical perfusion[26], also allows molecular imaging[27]. PET has been successfully used in patients with renovascular disease[28], renal allografts[29], and CKD[30]. The combined PET/CT modalities provides detailed morphology in addition to molecular function and is thus particularly powerful for assessments of renal perfusion and metabolism. Its niche appears to reside in renal cancer, but has also been applied in patients with obesity[31] or hypertension[32]. Additional studies are needed to test the clinical validity of this technique to improve the management and outcome of patients with CKD.

Ultra-small paramagnetic iron-oxide-based MRI can assess single-kidney blood volume[33], while non-CE MRI offers non-invasive measurements of both RBF and perfusion. Phase-contrast MRI measures blood flow velocity in individual vessels that occupy at least 16-pixels, to curtail partial volume errors[34], and allows computing RBF, alongside several derivative hemodynamic parameters. Although not routinely used in patients, several clinical studies show its potential to support diagnosis and monitoring the early-stage of chronic diseases like CKD, renovascular disease, and PKD[35]. Arterial spin-labelling (ASL) MRI uses magnetic labelling of water protons in arterial blood as an endogenous tracer to generate maps of regional perfusion. ASL, suited for repeated and longitudinal studies, shows clinical potential to detect early renal damage in ischemia-reperfusion injury, acute kidney injury, or renal transplantation, yet remains restricted to research settings[36]. Last, hyperpolarized ^{129}Xe-MRI has been recently proposed to depict human kidney tissue perfusion[37].

Color-Doppler ultrasonography is easily accessible, but user-dependent and technically challenging to make accurate measurements. CEUS can assess microvascular perfusion with satisfactory spatial resolution (Figure 2) and was applied in a variety of kidney diseases, including CKD, diabetic nephropathy, acute renal failure, and renal transplantation[2]. CEUS recently detected important reductions in cortical micro-perfusion in patients with moderate CKD, and perfusion increase following lower-salt intake[38]. Finally, ultrasound superb microvascular imaging[39] allows visualizing low-velocity and small-diameter blood vessel flow using advanced Doppler algorithms and filters to suppress noise caused by motion artifacts, and super-resolution imaging[40] noninvasively detects renal microvascular changes. Recent 3D-ultrasound advances may enable noninvasive and rapid measurement of renal perfusion with no CE[41], but still await clinical translation.

Function and metabolism

GFR.

99mTc-DTPA scintigraphy has been traditionally used to measure relative GFR, despite requiring 2-4-hour protocol and lower accuracy than alternative exogenous GFR measurement techniques. Dynamic CE (DCE)-MRI allows quantifying single-kidney GFR from time-indicator curves. DCE-MRI can assess renal function in patients with renal artery stenosis and urinary obstruction[42] and in living kidney donors[43], but not in transplant recipients, whose anatomical peculiarities confound standardization of arterial input function[44]. Moreover, DCE-MRI faces important challenges, including i) requirement for gadolinium-based agents, linked to adverse effects in patients with impaired renal function, ii) technical challenges like quantification of gadolinium concentration from signal intensity, spatial registration of the dynamic data and tissue segmentation, and iii) lack of standardization required for clinical practice, which inhibited its widespread clinical use. Importantly, however, new generation Group-II gadolinium-based contrast agents show a markedly improved safety profile[45]. CE-CT also provides single-kidney GFR from time-indicator curves[25], as iodine concentration is linearly-related to signal, but the need for contrast agents and radiation exposure restrict clinical application.

Tubular function.

99mTc-MAG3 scintigraphy allows studying tubular function and diagnosing tubular necrosis. Blood Oxygenation Level Dependent (BOLD) MRI, measuring tissue deoxyhemoglobin levels, allows assessing tubular function in-vivo but necessitates a tubule-specific pharmacological maneuver. Indeed, acute changes in oxygenation occur in humans in response to furosemide, and reduced response might reflect tubular damage[46]. Because furosemide does not affect RBF in healthy volunteers, it may help detect changes in renal oxygen consumption regardless of supply[47],

Solute transport.

Quantitative sodium (23Na)-MRI provides noninvasive quantification of tissue sodium concentration and corticomedullary gradient. Corticomedullary sodium gradient falls in kidney disease and grafts, whereas tissue sodium concentrations increase in diabetic, chronic, and acute kidney injury[48]. Although 23Na-MRI currently requires expensive hardware and software not routinely available on clinical MRI systems, it may become a noninvasive biomarker of physiological renal function and viability. Moreover, the ability to also assess potassium[49] opens new perspectives in renal physiological imaging.

Metabolism.

PET-derived uptake of [18F]fluorodeoxyglucose (FDG) is a powerful index of kidney metabolism[50], and ^{18}F-BCPP-BF uptake detects mitochondrial function in-vivo[27], but both are limited by radioactivity and low spatial resolution. Hyperpolarized-carbon-13-MRI is an emerging technique based on enzymatic conversion of injected hyperpolarized substrates, which provides both chemical and spatial information. Endogenous probes like pyruvate and urea, with no adverse effects, are particularly promising[51]. Hyperpolarized-MRI kidney studies have primarily focused on hypoxia or oxidative stress, potential unifying mechanisms for kidney disease. Recent clinical translation in oncology, in heart, liver, and brain disease[52] sets the stage for advances needed to turn hyperpolarized-MRI into a clinical tool.

Oxygenation

Oxygen consumption.

BOLD-MRI is the best-established imaging technique to monitor tissue oxygenation in humans, providing an indirect measure of partial oxygen pressure (pO2). BOLD-MRI may predict renal function decline, and provides powerful insight into the effects of drugs on kidney oxygenation[53]. In patients with asymmetric disease, single-kidney studies are particularly useful. Despite validation against direct measurement of tissue pO2 in animals, biological validation of BOLD-MRI in humans is warranted. Moreover, many factors including hydration, dietary salt intake, bowel gas, and carbogen and oxygen breathing could potentially affect BOLD-MRI and should be adequately standardized[53]. Concurrent measurements of RBF or perfusion may assist in result interpretation.

Ischemia.

Diffusion-weighted imaging (DWI)-MRI is capable of estimating ischemia/reperfusion injury delaying graft function[54], but not predicting renal artery revascularization success[55]. Very recent developments include hyperpolarized-[1-^{13}C]pyruvate imaging, allowing to evaluate metabolic status directly in ischemic kidneys[56] and MRI-CEST (chemical-exchange-saturation-transfer) pH-mapping to evaluate both acid-base homeostasis and renal filtration[57].

Viability.

Dynamic manganese-enhanced-MRI (MEMRI) allows tracing manganese uptake reflecting cellular viability. In ischemic mouse kidneys, MEMRI revealed decreased cellular viability[58]. This technique may afford noninvasive evaluation of renal viability, but is limited by toxicity that prohibits clinical translation.

Microstructure

Fibrosis.

Fibrosis can be assessed through its impact on renal functional (water diffusion, tissue hypoxia), structural (texture, contour), mechanical (stiffness), and molecular (elastin, macromolecule content) properties. Standard B-mode ultrasound is commonly used to detect kidney fibrosis, which increases cortical echogenicity, decreases its thickness, and alters its contour, although these are insensitive and nonspecific for fibrosis. Ultrasound strain-elastography is the first applied examination to measure kidney stiffness. UE has been widely used to assess liver fibrosis, in particular acoustic radiation force impulse (ARFI), measuring shear wave velocity[59], and shear wave elastography (SWE), and strongly correlates with kidney fibrosis in experimental models[60]. It improves fibrosis assessment in human kidneys, despite complex acoustic characteristics resulting from kidney heterogeneous histological structure and anisotropy[61]. Ultrasound-SWE, denoted by lower susceptibility to other factors and higher repeatability, is now the most widely used method, showing promise to investigate renal allografts, histopathology, or contrast-induced nephropathy. Recent exciting developments include real-time elastography[62]. Moreover, CEUS can evaluate tubular atrophy/interstitial fibrosis in IgA nephropathy[63]. Nevertheless, confounders and fibrosis-independent contributors to kidney stiffness, like RBF and complex tissue structure, remain to be teased out.

MR elastography (MRE)[64] detects increased stiffness with CKD[65] and allograft fibrosis[66], and may outperform UE in predicting graft loss[67]. T1/T2 mapping, susceptibility-weighted imaging, and magnetization-transfer imaging[68], are still at early stages of validation. To overcome the low specificity of non-CE-MRI, molecular MRI applies gadolinium-based probes specifically characterizing cellular processes[69], but is yet to enter clinical development[70]. CE-CT affords imaging of renal fibrosis[71], but due to application of ionizing radiation exposure and intra-arterial injections of nanoparticles, is limited to preclinical settings. Last, 99mTc-DMSA scintigraphy allows detecting renal scarring after acute pyelonephritis[72].

Microstructure.

DWI, by assessing tissue displacement of water molecules, is sensitive to alterations in the renal interstitium, cellular infiltration, or edema, perfusion and water handling in the tubular compartment[73]. Moreover, diffusion-tensor imaging (DTI) detects microstructural changes depending on the directionality of molecular motion. Magnetic-resonance relaxometry generates pixel-wise parametric maps of T1/T2 relaxation times reflecting specific tissue properties in kidney injury or graft dysfunction[74], and together with DWI successfully probed histopathologic microstructure in transplant recipients[75].

Interstitium

Inflammation and edema.

Several new imaging methods and probes detect cellular or molecular markers of kidney inflammation, yet most are still in the preclinical phase. Vascular leakage and edema can be visualized by MRI T1/T2 mapping[74], but changes in T1 are non-specific. CEUS detects renal inflammation employing microbubbles conjugated with molecules targeting endothelial inflammation markers[76]. The superparamagnetic iron-oxide (SPIO) MRI probe demonstrates kidney infiltration by macrophages[77], and when conjugated with molecules targeting tissue-bound complement C3 fragments can monitor kidney inflammation in animal models[69]. While some agents have reached regulatory approval, clinical evidence is still needed to translate SPIO-MRI into a clinical tool to probe inflammation.[78] 99mTc-OKT3 renal scintigraphy, identifying CD3-positive T-cells, may detect early rejection of renal allografts[79]. Finally, a recent study integrated CXCR4-targeted PET to detect leukocyte infiltrates, with MRI to localize them, in patients with complicated urinary tract infections, informing on the source and extension of local infection[80].

Abscess/infection.

Imaging techniques play a key role in the diagnosis of infectious complications[81,82]. Plain radiography illustrates peri-renal gas in emphysematous pyelonephritis or abscess and calcification in end-stage renal tuberculosis. Ultrasound is often used as screening modality and guiding interventions, portraying kidney mobility, enlargement, parenchyma thickening, and corticomedullary differentiation. Yet, CT is the gold-standard technique for diagnosis and assessment of acute pyelonephritis and to resolve uncertain ultrasound findings. MRI is more sensitive and specific than CT, but not commonly used as first-line, because of high cost and lower accessibility. However, it is helpful in pregnancy and patients with contraindication to iodinated contrast[83,84]. DWI is more sensitive than sonography to detect infected renal segments during acute pyelonephritis and to differentiate abscesses from cysts. Finally, [18F]FDG PET/CT proved useful in the diagnosis of renal and hepatic cyst infection in patients with PKD[85].

Unmet targets and future directions

Since the range of renal imaging techniques is broad and varied, the choice should be driven by the clinical question and specific underlying pathological mechanism, considering contraindications and possible adverse effects (Tables 1–2). Integration of different modalities providing complementary information will likely bestow the greatest insight into renal pathophysiology. In this respect, multiparametric MRI (Figure 3) may represent the lowest-hanging fruit[46,86], with MRI-fingerprinting being a promising development[87]. Moreover, PET/MRI, although currently focusing on oncological applications, uniquely combines structural, functional and molecular imaging[88] (Figure 4) with considerably lower radiation exposure than PET/CT[89]. Tremendous advances made in clinical renal imaging so far pave the way for exciting future developments.

For example, assessment of the renal microcirculation in-vivo would provide insight on progression of renal microvascular disease and regeneration. Super microvascular imaging[39] and super-resolution ultrasound microvessel imaging[40] may be useful for this purpose. Determination of nephron number and glomerular size in living humans in-vivo remains an unmet target, and cationized-ferritin-enhanced MRI remains to be developed for clinical application[90]. The ability to discern intra-renal cellular composition would also illuminate renal pathophysiology and disease mechanisms.

Artificial intelligence is catching on very quickly in imaging. Methods based on deep-learning have provided excellent automatic 3D segmentation of the kidney using deep neural networks[91], enhance ultrasound image quality[92], and score kidney stones on non-CE CT[93]. Moreover, texture analysis based on multiple MRI sequences show promise to assess early renal dysfunction[94]. This is just the beginning, and rapid progress is anticipated.

Clinical translation.

Kidney imaging biomarkers can help address the urgent need to improve kidney disease management and clinical trials outcomes. Among all available techniques, the most auspicious might be ultrasound-based due to its non-invasiveness, ease of use, and gains from rapid technological progress. Additionally, various MR modalities are favorable for mechanism-based investigation of kidney tissue, in particular DWI, BOLD, ASL, MTI and 23-Na techniques.

Imaging biomarkers could help tailor therapy founded on in-depth understanding of disease mechanisms, enrich clinical trials, and identify patients suitable for novel treatments. Moreover, imaging biomarkers suited for serial applications could monitor response to treatment.

Despite encouraging research results, several factors may prohibit advanced renal imaging techniques from achieving regulatory qualification and routine clinical use. For example, research studies emphasize analytical inferences based on group differences, whereas clinical practice needs to deliver to individual diagnostic and treatment decisions. This discrepancy might be addressed by applying machine learning methods to make inferences based on individual structural or functional imaging data[95]. While complex, time-consuming, and expertise-demanding data analysis might forbid rapid clinical decision-making, these might be thwarted by implementation of automated, user-friendly software tools. Amplified volume and complexity of imaging data could be circumvented by developing powerful data archiving and software tools. Furthermore, standardization of data acquisition and analysis may avoiding repetition, unlock silos, and thereby consolidate the discovery and validation powers of multiple groups.

In summary, major recent advances and the rapid ongoing progress in key tools for clinical kidney imaging are preparing the grounds for future incorporation of imaging biomarkers in clinical practice. Rapid gains in resolution and machine learning techniques may allow unprecedented insights into kidney physiology and pathology. The imaging biomarker roadmap recently developed for cancer[96] provides a useful guide for clinical translation. Parallel tracks of technical validation, biological/clinical validation, and assessment of costeffectiveness; imaging biomarker standardization; and multicenter studies are needed to cross translational gaps.

Acknowledgments

Funding Sources

Partly supported by the National Institutes of Health (DK122734, DK120292, and AG062104).

References

1. Klibanov AL. Ultrasound Contrast: Gas Microbubbles in the Vasculature. Invest Radiol. 2021;56(1):50–61. doi:10.1097/RLI.0000000000000733 [PubMed: 33181574]
2. Drudi FM, Cantisani V, Granata A, et al. Multiparametric ultrasound in the evaluation of kidney disease in elderly. J Ultrasound. 2020;23(2):115–126. doi:10.1007/s40477-019-00390-5 [PubMed: 31197634]
3. Qi R, Yang C, Zhu T. Advances of Contrast-Enhanced Ultrasonography and Elastography in Kidney Transplantation: From Microscopic to Microcosmic. Ultrasound Med Biol. Published online 10 31, 2020. doi:10.1016/j.ultrasmedbio.2020.07.025
4. Selby NM, Blankestijn PJ, Boor P, et al. Magnetic resonance imaging biomarkers for chronic kidney disease: a position paper from the European Cooperation in Science and Technology Action PARENCHIMA. Nephrol Dial Transplant. 2018;33(suppl_2):ii4–ii14. doi:10.1093/ndt/gfy152 [PubMed: 30137584]
5. Keramida G, James JM, Prescott MC, Peters AM. Pitfalls and Limitations of Radionuclide Renal Imaging in Adults. Semin Nucl Med. 2015;45(5):428–439. doi:10.1053/j.semnuclmed.2015.02.008 [PubMed: 26278854]
6. Grantham JJ, Torres VE. The importance of total kidney volume in evaluating progression of polycystic kidney disease. Nat Rev Nephrol. 2016;12(11):667–677. doi:10.1038/nrneph.2016.135 [PubMed: 27694979]
7. Issa N, Lopez CL, Denic A, et al. Kidney Structural Features from Living Donors Predict Graft Failure in the Recipient. J Am Soc Nephrol. 2020;31(2):415–423. doi:10.1681/ASN.2019090964 [PubMed: 31974271]
8. Duan X, Rule AD, Elsherbiny H, et al. Automated assessment of renal cortical surface roughness from computerized tomography images and its association with age. Acad Radiol. 2014;21(11):1441–1445. doi:10.1016/j.acra.2014.05.014 [PubMed: 25086950]
9. Lin P, Min Z, Wei G, Lei H, Feifei Z, Yunfei Z. Volumetric evaluation of renal sinus adipose tissue on computed tomography images in bilateral nephrolithiasis patients. Int Urol Nephrol. 2020;52(6):1027–1034. doi:10.1007/s11255-020-02395-0 [PubMed: 32006179]
10. Notohamiprodjo M, Goepfert M, Will S, et al. Renal and renal sinus fat volumes as quantified by magnetic resonance imaging in subjects with prediabetes, diabetes, and normal glucose tolerance. PLoS One. 2020;15(2):e0216635. doi:10.1371/journal.pone.0216635 [PubMed: 32074103]
11. Fang Y, Xu Y, Yang Y, Liu C, Zhao D, Ke J. The Relationship between Perirenal Fat Thickness and Reduced Glomerular Filtration Rate in Patients with Type 2 Diabetes. J Diabetes Res. 2020;2020:6076145. doi:10.1155/2020/6076145 [PubMed: 32685560]
12. Rule AD, Lieske JC, Pais VMJ. Management of Kidney Stones in 2020. JAMA. 2020;323(19):1961–1962. doi:10.1001/jama.2020.0662 [PubMed: 32191284]
13. Ferrero A, Gutjahr R, Halaweish AF, Leng S, McCollough CH. Characterization of Urinary Stone Composition by Use of Whole-body, Photon-counting Detector CT. Acad Radiol. 2018;25(10):1270–1276. doi:10.1016/j.acra.2018.01.007 [PubMed: 29454545]
14. Mussmann B, Hardy M, Jung H, Ding M, Osther PJ, Graumann O. Can Dual Energy CT with Fast kV-Switching Determine Renal Stone Composition Accurately? Acad Radiol. Published online 3 23, 2020. doi:10.1016/j.acra.2020.02.007
15. Fried JG, Morgan MA. Renal Imaging: Core Curriculum 2019. Am J Kidney Dis. 2019;73(4):552–565. doi: 10.1053/j.ajkd.2018.12.029 [PubMed: 30777633]

16. Finn JP. Contrast-enhanced MR Angiography without Gadolinium. Radiology. 2020;297(1):223–224. doi: 10.1148/radiol.2020202574 [PubMed: 32697168]
17. Dillman JR, Trout AT, Smith EA. MR urography in children and adolescents: techniques and clinical applications. Abdom Radiol (NY). 2016;41(6): 1007–1019. doi:10.1007/s00261-016-0669-z [PubMed: 26915088]
18. Edelman RR, Koktzoglou I. Noncontrast MR angiography: An update. J Magn Reson Imaging. 2019;49(2):355–373. doi:10.1002/jmri.26288 [PubMed: 30566270]
19. Scholtes RA, Nguyen ITN, van Bommel EJM, et al. Glucosuria Interferes With Measurement of Effective Renal Plasma Flow Using para-Aminohippuric Acid, With a Focus on SGLT2 Inhibitors. Kidney IntRep. 2020;5(11):2052–2054. doi: 10.1016/j.ekir.2020.09.002
20. Volkan-Salanci B, Erbas B. Imaging in Renal Transplants: An Update. Semin Nucl Med. Published online 1 20, 2021. doi:10.1053/j.semnuclmed.2020.12.011
21. Jaksić E, Artiko V, Beatović S, et al. Clinical investigations of 99mTc-p-aminohippuric acid as a new renal agent. Nncl Med Commun. 2009;30(1):76–81. doi:10.1097/mnm.0b013e328314b8bc
22. Cichocki P, Filipczak K, Adamczewski Z, Kuśmierek J, Plachcińska A. Assessment of Renal Function Based on Dynamic Scintigraphy Parameters in the Diagnosis of Obstructive Uro/Nephropathy. J Clin Med. 2021;10(3). doi:10.3390/jcm10030529
23. Abumoawad A, Saad A, Ferguson CM, et al. In a Phase 1a escalating clinical trial, autologous mesenchymal stem cell infusion for renovascular disease increases blood flow and the glomerular filtration rate while reducing inflammatory biomarkers and blood pressure. Kidney Int. 2020;97(4):793–804. doi: 10.1016/j.kint.2019.11.022 [PubMed: 32093917]
24. Saad A, Herrmann SMS, Eirin A, et al. Phase 2a Clinical Trial of Mitochondrial Protection (Elamipretide) During Stent Revascularization in Patients With Atherosclerotic Renal Artery Stenosis. Circ Cardiovasc Interv. 2017; 10(9). doi:10.1161/CIRCINTERVENTIONS.117.005487
25. Kwon SH, Saad A, Herrmann SM, Textor SC, Lerman LO. Determination of Single-Kidney Glomerular Filtration Rate in Human Subjects by Using CT. Radiology. 2015;276(2):490–498. doi:10.1148/radiol.2015141892 [PubMed: 25848903]
26. Rahman M, Watabe H, Shidahara M, et al. Renal statistical map for positron emission tomography with [O-15] water. Am J Nucl Med Mol Imaging. 2019;9(4):193–202. [PubMed: 31516765]
27. Saeki S, Ohba H, Ube Y, et al. Positron emission tomography imaging of renal mitochondria is a powerful tool in the study of acute and progressive kidney disease models. Kidney Int. 2020;98(1):88–99. doi:10.1016/j.kint.2020.02.024 [PubMed: 32471638]
28. Päivärinta J, Koivuviita N, Oikonen V, et al. The renal blood flow reserve in healthy humans and patients with atherosclerotic renovascular disease measured by positron emission tomography using [(15)O]H(2)O. EJNMMI Res. 2018;8(1):45. doi:10.1186/s13550-018-0395-3 [PubMed: 29892792]
29. Pawelski H, Schnöckel U, Kentrup D, Grabner A, Schäfers M, Reuter S. SPECT- and PET-based approaches for noninvasive diagnosis of acute renal allograft rejection. Biomed Res Int. 2014;2014:874785. doi:10.1155/2014/874785 [PubMed: 24804257]
30. Juillard L, Janier MF, Fouque D, et al. Dynamic renal blood flow measurement by positron emission tomography in patients with CRF. Am J Kidney Dis. 2002;40(5):947–954. doi:10.1053/ajkd.2002.36325 [PubMed: 12407639]
31. Rebelos E, Dadson P, Oikonen V, et al. Renal hemodynamics and fatty acid uptake: effects of obesity and weight loss. Am J Physiol Endocrinol Metab. 2019;317(5):E871–E878. doi:10.1152/ajpendo.00135.2019 [PubMed: 31550182]
32. Assersen KB, Høilund-Carlsen PF, Olsen MH, et al. The exaggerated natriuresis of essential hypertension occurs independently of changes in renal medullary blood flow. Acta Physiol (Oxf). 2019;226(3):e13266. doi:10.1111/apha.13266 [PubMed: 30770642]
33. Niendorf T, Seeliger E, Cantow K, Flemming B, Waiczies S, Pohlmann A. Probing renal blood volume with magnetic resonance imaging. Acta Physiol (Oxf). 2020;228(4):e13435. doi:10.1111/apha.13435 [PubMed: 31876349]
34. Nayak KS, Nielsen J-F, Bernstein MA, et al. Cardiovascular magnetic resonance phase contrast imaging. J Cardiovasc Magn Reson. 2015;17(1):71. doi:10.1186/s12968-015-0172-7 [PubMed: 26254979]

35. Villa G, Ringgaard S, Hermann I, et al. Phase-contrast magnetic resonance imaging to assess renal perfusion: a systematic review and statement paper. MAGMA. 2020;33(1):3–21. doi:10.1007/s10334-019-00772-0 [PubMed: 31422518]

36. Odudu A, Nery F, Harteveld AA, et al. Arterial spin labelling MRI to measure renal perfusion: a systematic review and statement paper. Nephrol Dial Transplant. 2018;33(suppl_2):ii15–ii21. doi:10.1093/ndt/gfy180 [PubMed: 30137581]

37. Chacon-Caldera J, Maunder A, Rao M, et al. Dissolved hyperpolarized xenon-129 MRI in human kidneys. Magn Reson Med. 2020;83(1):262–270. doi:10.1002/mrm.27923 [PubMed: 31400040]

38. Garessus J, Brito W, Loncle N, et al. Cortical perfusion as assessed with contrast-enhanced ultrasound is lower in patients with chronic kidney disease than in healthy subjects but increases under low salt conditions. Nephrol Dial Transplant. Published online 1 11, 2021. doi:10.1093/ndt/gfab001

39. Gao J, Thai A, Erpelding T. Comparison of superb microvascular imaging to conventional color Doppler ultrasonography in depicting renal cortical microvasculature. Clin Imaging. 2019;58:90–95. doi:10.1016/j.clinimag.2019.06.011 [PubMed: 31284178]

40. Chen Q, Yu J, Rush BM, Stocker SD, Tan RJ, Kim K. Ultrasound super-resolution imaging provides a noninvasive assessment of renal microvasculature changes during mouse acute kidney injury. Kidney Int. 2020;98(2):355–365. doi:10.1016/j.kint.2020.02.011 [PubMed: 32600826]

41. Welsh AW, Fowlkes JB, Pinter SZ, et al. Three-dimensional US Fractional Moving Blood Volume: Validation of Renal Perfusion Quantification. Radiology. 2019;293(2):460–468. doi:10.1148/radiol.2019190248 [PubMed: 31573404]

42. Zeng M, Cheng Y, Zhao B. Measurement of single-kidney glomerular filtration function from magnetic resonance perfusion renography. Eur J Radiol. 2015;84(8):1419–1423. doi:10.1016/j.ejrad.2015.05.009 [PubMed: 26032130]

43. Eikefjord E, Andersen E, Hodneland E, Svarstad E, Lundervold A, Rørvik J. Quantification of Single-Kidney Function and Volume in Living Kidney Donors Using Dynamic Contrast-Enhanced MRI. AJR Am J Roentgenol. 2016;207(5):1022–1030. doi:10.2214/AJR.16.16168 [PubMed: 27557401]

44. Taton B, De La Faille R, Asselineau J, et al. A prospective comparison of dynamic contrast-enhanced MRI and (51)Cr-EDTA clearance for glomerular filtration rate measurement in 42 kidney transplant recipients. Eur J Radiol. 2019;117:209–215. doi:10.1016/j.ejrad.2019.02.002 [PubMed: 31221527]

45. Woolen SA, Shankar PR, Gagnier JJ, MacEachern MP, Singer L, Davenport MS. Risk of Nephrogenic Systemic Fibrosis in Patients With Stage 4 or 5 Chronic Kidney Disease Receiving a Group II Gadolinium-Based Contrast Agent: A Systematic Review and Metaanalysis. JAMA Intern Med. 2020;180(2):223–230. doi:10.1001/jamainternmed.2019.5284 [PubMed: 31816007]

46. Prasad PV, Li L-P, Thacker JM, et al. Cortical Perfusion and Tubular Function as Evaluated by Magnetic Resonance Imaging Correlates with Annual Loss in Renal Function in Moderate Chronic Kidney Disease. Am J Nephrol. 2019;49(2):114–124. doi:10.1159/000496161 [PubMed: 30669143]

47. Haddock B, Larsson HBW, Francis S, Andersen UB. Human renal response to furosemide: Simultaneous oxygenation and perfusion measurements in cortex and medulla. Acta Physiol (Oxf). 2019;227(1):e13292. doi:10.1111/apha.13292 [PubMed: 31046189]

48. Qirjazi E, Salerno FR, Akbari A, et al. Tissue sodium concentrations in chronic kidney disease and dialysis patients by lower leg sodium-23 magnetic resonance imaging. Nephrol Dial Transplant. Published online 4 6, 2020. doi:10.1093/ndt/gfaa036

49. Gast LV, Völker S, Utzschneider M, et al. Combined imaging of potassium and sodium in human skeletal muscle tissue at 7 T. Magn Reson Med. 2021;85(1):239–253. doi:10.1002/mrm.28428 [PubMed: 32869364]

50. Hanssen O, Weekers L, Lovinfosse P, et al. Diagnostic yield of (18) F-FDG PET/CT imaging and urinary CXCL9/creatinine levels in kidney allograft subclinical rejection. Am J Transplant. 2020;20(5):1402–1409. doi:10.1111/ajt.15742 [PubMed: 31841263]

51. Wang ZJ, Ohliger MA, Larson PEZ, et al. Hyperpolarized (13)C MRI: State of the Art and Future Directions. Radiology. 2019;291(2):273–284. doi:10.1148/radiol.2019182391 [PubMed: 30835184]
52. Schroeder M, Laustsen C. Imaging oxygen metabolism with hyperpolarized magnetic resonance: a novel approach for the examination of cardiac and renal function. Biosci Rep. 2017;37(1). doi:10.1042/BSR20160186
53. Pruijm M, Mendichovszky IA, Liss P, et al. Renal blood oxygenation level-dependent magnetic resonance imaging to measure renal tissue oxygenation: a statement paper and systematic review. Nephrol Dial Transplant. 2018;33(suppl_2):ii22–ii28. doi:10.1093/ndt/gfy243 [PubMed: 30137579]
54. Hashim E, Yuen DA, Kirpalani A. Reduced Flow in Delayed Graft Function as Assessed by IVIM Is Associated With Time to Recovery Following Kidney Transplantation. J Magn Reson Imaging. Published online 6 29, 2020. doi:10.1002/jmri.27245
55. Ferguson CM, Eirin A, Abumoawad A, et al. Renal fibrosis detected by diffusion-weighted magnetic resonance imaging remains unchanged despite treatment in subjects with renovascular disease. Sci Rep. 2020;10(1):16300. doi:10.1038/s41598-020-73202-0 [PubMed: 33004888]
56. Nielsen PM, Qi H, Bertelsen LB, Laustsen C. Metabolic reprogramming associated with progression of renal ischemia reperfusion injury assessed with hyperpolarized [1-(13)C]pyruvate. Sci Rep. 2020;10(1):8915. doi:10.1038/s41598-020-65816-1 [PubMed: 32488151]
57. Irrera P, Consolino L, Cutrin JC, Zöllner FG, Longo DL. Dual assessment of kidney perfusion and pH by exploiting a dynamic CEST-MRI approach in an acute kidney ischemia-reperfusion injury murine model. NMR Biomed. 2020;33(6):e4287. doi:10.1002/nbm.4287 [PubMed: 32153058]
58. Jiang K, Tang H, Mishra PK, Macura SI, Lerman LO. A rapid T(1) mapping method for assessment of murine kidney viability using dynamic manganese-enhanced magnetic resonance imaging. Magn Reson Med. 2018;80(1):190–199. doi:10.1002/mrm.27025 [PubMed: 29193339]
59. Bruno C, Minniti S, Bucci A, Pozzi Mucelli R. ARFI: from basic principles to clinical applications in diffuse chronic disease-a review. Insights Imaging. 2016;7(5):735–746. doi:10.1007/s13244-016-0514-5 [PubMed: 27553006]
60. Moon SK, Kim SY, Cho JY, Kim SH. Quantification of kidney fibrosis using ultrasonic shear wave elastography: experimental study with a rabbit model. J Ultrasound Med. 2015;34(5):869–877. doi:10.7863/ultra.34.5.869 [PubMed: 25911705]
61. Wang L Applications of acoustic radiation force impulse quantification in chronic kidney disease: a review. Ultrasonography. 2016;35(4):302–308. doi:10.14366/usg.16026 [PubMed: 27599890]
62. Yang J-R, La Q, Ding X-M, Song Y, Wang Y-Y. Using real-time sound touch elastography to monitor changes in transplant kidney elasticity. Clin Radiol. 2020;75(12):963.e1–963.e6. doi:10.1016/j.crad.2020.08.013
63. Yang W, Mou S, Xu Y, et al. Contrast-enhanced ultrasonography for assessment of tubular atrophy/ interstitial fibrosis in immunoglobulin A nephropathy: a preliminary clinical study. Abdom Radiol (NY). 2018;43(6):1423–1431. doi:10.1007/s00261-017-1301-6 [PubMed: 29110052]
64. Serai SD, Yin M. MR Elastography of the Abdomen: Basic Concepts. Methods Mol Biol. 2021;2216:301–323. doi:10.1007/978-1-0716-0978-1_18 [PubMed: 33476008]
65. Han JH, Ahn J-H, Kim J-S. Magnetic resonance elastography for evaluation of renal parenchyma in chronic kidney disease: a pilot study. Radiol Med. 2020;125(12):1209–1215. doi:10.1007/ s11547-020-01210-1 [PubMed: 32367323]
66. Kirpalani A, Hashim E, Leung G, et al. Magnetic Resonance Elastography to Assess Fibrosis in Kidney Allografts. Clin J Am Soc Nephrol. 2017;12(10):1671–1679. doi:10.2215/CJN.01830217 [PubMed: 28855238]
67. Kennedy P, Bane O, Hectors SJ, et al. Magnetic resonance elastography vs. point shear wave ultrasound elastography for the assessment of renal allograft dysfunction. Eur J Radiol. 2020;130:109180. doi:10.1016/j.ejrad.2020.109180 [PubMed: 32736305]
68. Afarideh M, Jiang K, Ferguson CM, Woollard JR, Glockner JF, Lerman LO. Magnetization Transfer Imaging Predicts Porcine Kidney Recovery After Revascularization of Renal Artery Stenosis. Invest Radiol. 2021;56(2):86–93. doi:10.1097/RLI.0000000000000711 [PubMed: 33405430]

69. Sun Q, Baues M, Klinkhammer BM, et al. Elastin imaging enables noninvasive staging and treatment monitoring of kidney fibrosis. Sci Transl Med. 2019;11(486). doi:10.1126/scitranslmed.aat4865
70. Caroli A, Remuzzi A, Remuzzi G. Does MRI trump pathology? A new era for staging and monitoring of kidney fibrosis. Kidney Int. 2020;97(3):442–444. doi:10.1016/j.kint.2019.10.008 [PubMed: 31902648]
71. Zhu X-Y, Zou X, Mukherjee R, et al. Targeted Imaging of Renal Fibrosis Using Antibody-Conjugated Gold Nanoparticles in Renal Artery Stenosis. Invest Radiol. 2018;53(10):623–628. doi:10.1097/RLI.0000000000000476 [PubMed: 29727402]
72. Sarikaya I, Sarikaya A. Current Status of Radionuclide Renal Cortical Imaging in Pyelonephritis. J Nucl Med Technol. 2019;47(4):309–312. doi:10.2967/jnmt.119.227942 [PubMed: 31182659]
73. Caroli A, Schneider M, Friedli I, et al. Diffusion-weighted magnetic resonance imaging to assess diffuse renal pathology: a systematic review and statement paper. Nephrol Dial Transplant. 2018;33(suppl_2):ii29–ii40. doi:10.1093/ndt/gfy163 [PubMed: 30137580]
74. Wolf M, de Boer A, Sharma K, et al. Magnetic resonance imaging T1- and T2-mapping to assess renal structure and function: a systematic review and statement paper. Nephrol Dial Transplant. 2018;33(suppl_2):ii41–ii50. doi:10.1093/ndt/gfy198 [PubMed: 30137583]
75. Adams LC, Bressem KK, Scheibl S, et al. Multiparametric Assessment of Changes in Renal Tissue after Kidney Transplantation with Quantitative MR Relaxometry and Diffusion-Tensor Imaging at 3 T. J Clin Med. 2020;9(5). doi:10.3390/jcm9051551
76. Hoyt K, Warram JM, Wang D, Ratnayaka S, Traylor A, Agarwal A. Molecular Ultrasound Imaging of Tissue Inflammation Using an Animal Model of Acute Kidney Injury. Mol Imaging Biol. 2015;17(6):786–792. doi:10.1007/s11307-015-0860-6 [PubMed: 25905474]
77. Hauger O, Grenier N, Deminère C, et al. USPIO-enhanced MR imaging of macrophage infiltration in native and transplanted kidneys: initial results in humans. Eur Radiol. 2007;17(11):2898–2907. doi:10.1007/s00330-007-0660-8 [PubMed: 17929025]
78. Wáng YXJ, Idée J-M. A comprehensive literatures update of clinical researches of superparamagnetic resonance iron oxide nanoparticles for magnetic resonance imaging. Quant Imaging Med Surg. 2017;7(1):88–122. doi:10.21037/qims.2017.02.09 [PubMed: 28275562]
79. Martins FPP, Souza SAL, Gonçalves RT, Fonseca LMB, Gutfilen B. Preliminary results of [99mTc]OKT3 scintigraphy to evaluate acute rejection in renal transplants. Transplant Proc. 2004;36(9):2664–2667. doi:10.1016/j.transproceed.2004.09.085 [PubMed: 15621118]
80. Derlin T, Gueler F, Bräsen JH, et al. Integrating MRI and Chemokine Receptor CXCR4-Targeted PET for Detection of Leukocyte Infiltration in Complicated Urinary Tract Infections After Kidney Transplantation. J Nucl Med. 2017;58(11):1831–1837. doi:10.2967/jnumed.117.193037 [PubMed: 28450555]
81. Zulfiqar M, Ubilla CV, Nicola R, Menias CO. Imaging of Renal Infections and Inflammatory Disease. Radiol Clin North Am. 2020;58(5):909–923. doi:10.1016/j.rcl.2020.05.004 [PubMed: 32792123]
82. Enikeev DV, Glybochko P, Alyaev Y, Enikeev M, Rapoport L. Imaging technologies in the diagnosis and treatment of acute pyelonephritis. Urologia. 2017;84(3):179–184. doi:10.5301/uj.5000234 [PubMed: 28525662]
83. Das CJ, Ahmad Z, Sharma S, Gupta AK. Multimodality imaging of renal inflammatory lesions. World J Radiol. 2014;6(11):865–873. doi:10.4329/wjr.v6.i11.865 [PubMed: 25431641]
84. Rubilotta E, Balzarro M, Lacola V, Sarti A, Porcaro AB, Artibani W. Current clinical management of renal and perinephric abscesses: a literature review. Urologia. 2014;81(3):144–147. doi:10.5301/urologia.5000044 [PubMed: 24474535]
85. Pijl JP, Glaudemans AWJM, Slart RHJA, Kwee TC. (18)F-FDG PET/CT in Autosomal Dominant Polycystic Kidney Disease Patients with Suspected Cyst Infection. J Nucl Med. 2018;59(11):1734–1741. doi:10.2967/jnumed.117.199448 [PubMed: 29653972]
86. Buchanan CE, Mahmoud H, Cox EF, et al. Quantitative assessment of renal structural and functional changes in chronic kidney disease using multi-parametric magnetic resonance imaging. Nephrol Dial Transplant. 2020;35(6):955–964. doi:10.1093/ndt/gfz129 [PubMed: 31257440]

87. Hermann I, Chacon-Caldera J, Brumer I, et al. Magnetic resonance fingerprinting for simultaneous renal T(1) and T2* mapping in a single breath-hold. Magn Reson Med. 2020;83(6): 1940–1948. doi:10.1002/mrm.28160 [PubMed: 31900983]
88. Suarez-Weiss KE, Herold A, Gervais D, et al. Hybrid imaging of the abdomen and pelvis. Radiologe. 2020;60(Suppl 1):80–89. doi:10.1007/s00117-020-00661-x [PubMed: 32424463]
89. Ward RD, Amorim B, Li W, et al. Abdominal and pelvic (18)F-FDG PET/MR: a review of current and emerging oncologic applications. Abdom Radiol (NY). Published online 9 19, 2020. doi:10.1007/s00261-020-02766-2
90. Charlton JR, Xu Y, Wu T, et al. Magnetic resonance imaging accurately tracks kidney pathology and heterogeneity in the transition from acute kidney injury to chronic kidney disease. Kidney Int. 2021;99(1):173–185. doi:10.1016/j.kint.2020.08.021 [PubMed: 32916180]
91. Heller N, Isensee F, Maier-Hein KH, et al. The state of the art in kidney and kidney tumor segmentation in contrast-enhanced CT imaging: Results of the KiTS19 challenge. Med Image Anal. 2020;67:101821. doi:10.1016/j.media.2020.101821 [PubMed: 33049579]
92. Yi J, Kang HK, Kwon J-H, et al. Technology trends and applications of deep learning in ultrasonography: image quality enhancement, diagnostic support, and improving workflow efficiency. Ultrasonography. Published online 9 14, 2020. doi:10.14366/usg.20102
93. Cui Y, Sun Z, Ma S, et al. Automatic Detection and Scoring of Kidney Stones on Noncontrast CT Images Using S.T.O.N.E. Nephrolithometry: Combined Deep Learning and Thresholding Methods. Mol Imaging Biol. Published online 10 27, 2020. doi:10.1007/s11307-020-01554-0
94. Ding J, Xing Z, Jiang Z, et al. Evaluation of renal dysfunction using texture analysis based on DWI, BOLD, and susceptibility-weighted imaging. Eur Radiol. 2019;29(5):2293–2301. doi:10.1007/s00330-018-5911-3 [PubMed: 30560361]
95. Scarpazza C, Miolla A, Zampieri I, et al. Translational Application of a Neuro-Scientific Multi-Modal Approach Into Forensic Psychiatric Evaluation: Why and How? Front Psychiatry. 2021;12:597918. doi:10.3389/fpsyt.2021.597918 [PubMed: 33613339]
96. O'Connor JPB, Aboagye EO, Adams JE, et al. Imaging biomarker roadmap for cancer studies. Nat Rev Clin Oncol. 2017;14(3):169–186. doi:10.1038/nrclinonc.2016.162 [PubMed: 27725679]

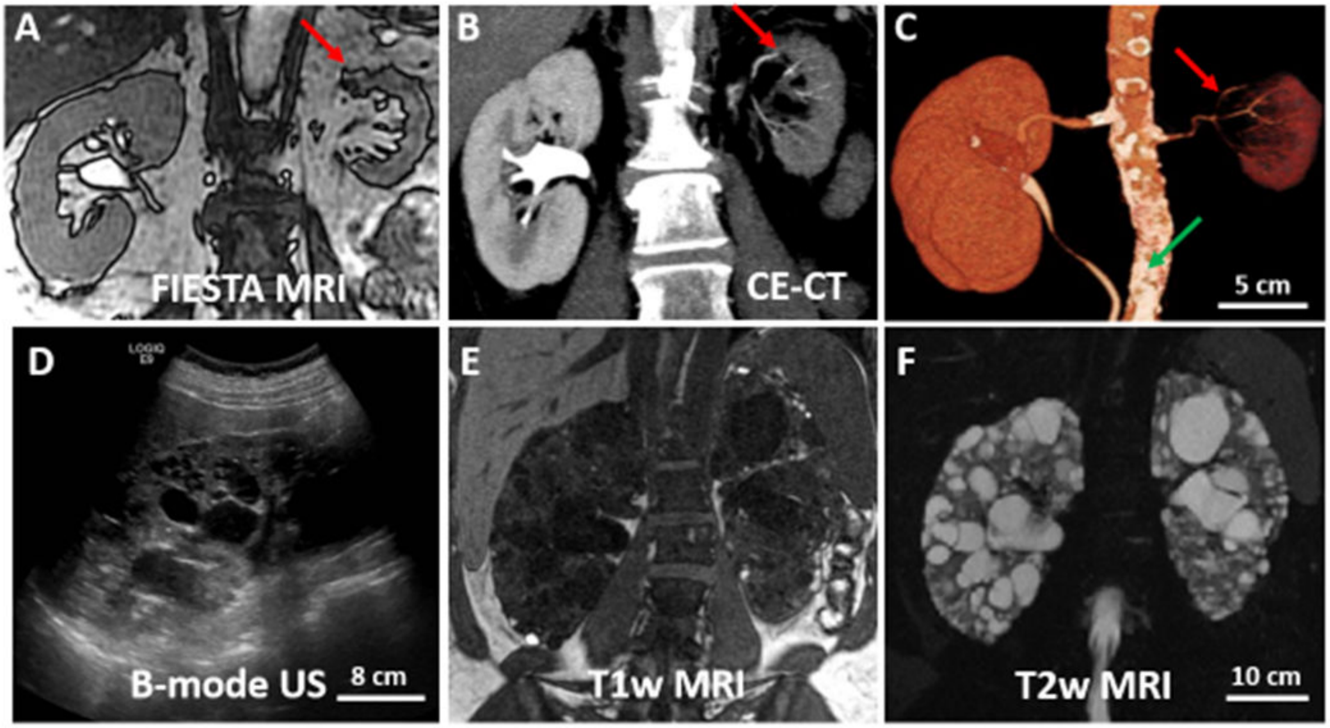

Figure 1. Anatomical imaging of the kidney in human subjects.

Top: Coronal 3D Fast Imaging Employing Steady-state Acquisition (FIESTA) anatomical MRI image (A); Co-registered, coronal (contrast-enhanced; CE) 3D CT image (B); and Maximum-Intensity-Projection reconstructed CT image (C) in the same human subject with asymmetric kidneys due to left renal artery stenosis. Both modalities demonstrate clearly a visibly shrunk and less perfused stenotic kidney (red arrow) compared to the contra-lateral kidney. CT also shows aortic calcifications (green arrow). **Bottom:** B-mode US image (D) and anatomical MR images obtained by T1-weighted (E) and T2-weighted (F) sequences in the same human patient with autosomal dominant polycystic kidney disease. Both US and MRI techniques illustrate the presence of echogenic and fluid-filled cysts in the kidney parenchyma.

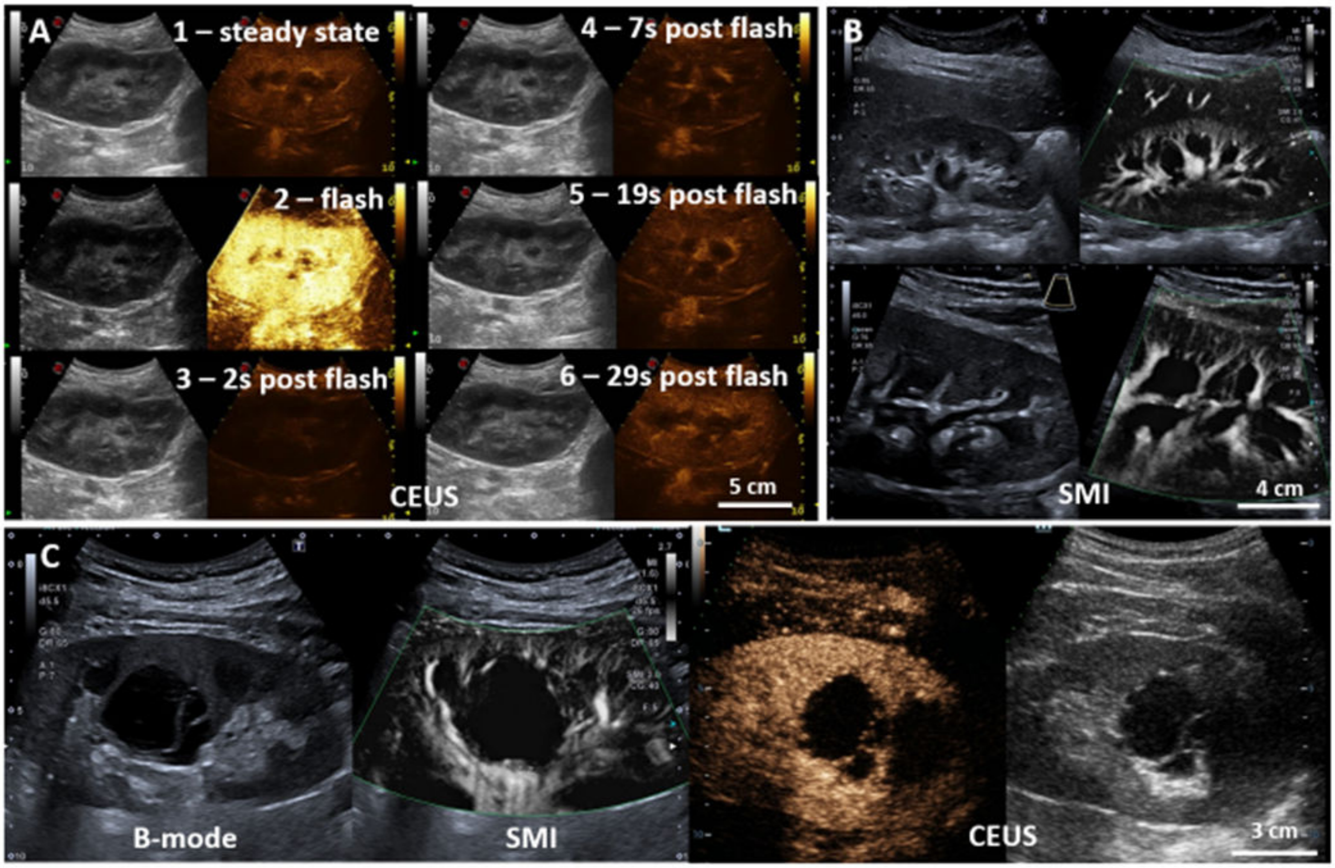

Figure 2. Latest ultrasound developments in the human kidney.

A) Assessment of tissue perfusion by contrast-enhanced ultrasound (CEUS) in a human transplanted kidney. After continuous infusion of the microbubble contrast agent at a constant rate, a steady state microbubble concentration is reached in the kidney. At that time, a short ultrasound pulse with a very high mechanical index (‘flash’) is generated, resulting in almost complete destruction of the contrast agent microbubbles in the imaging plane. Post-flash images are serially acquired, and perfusion is assessed by the post-flash replenishment kinetics of the volume of microbubbles. B) representative superb microvascular imaging (SMI) ultrasound images of the kidney. Using advanced Doppler algorithms and filters, SMI can suppress noise caused by motion artifacts, without removing the weak signal arising from small vessel blood flow, thereby allowing investigation of the renal microvasculature with no need for contrast media. C) ultrasound investigation of a complex kidney cyst, by B-mode, SMI (left) and CEUS (right).

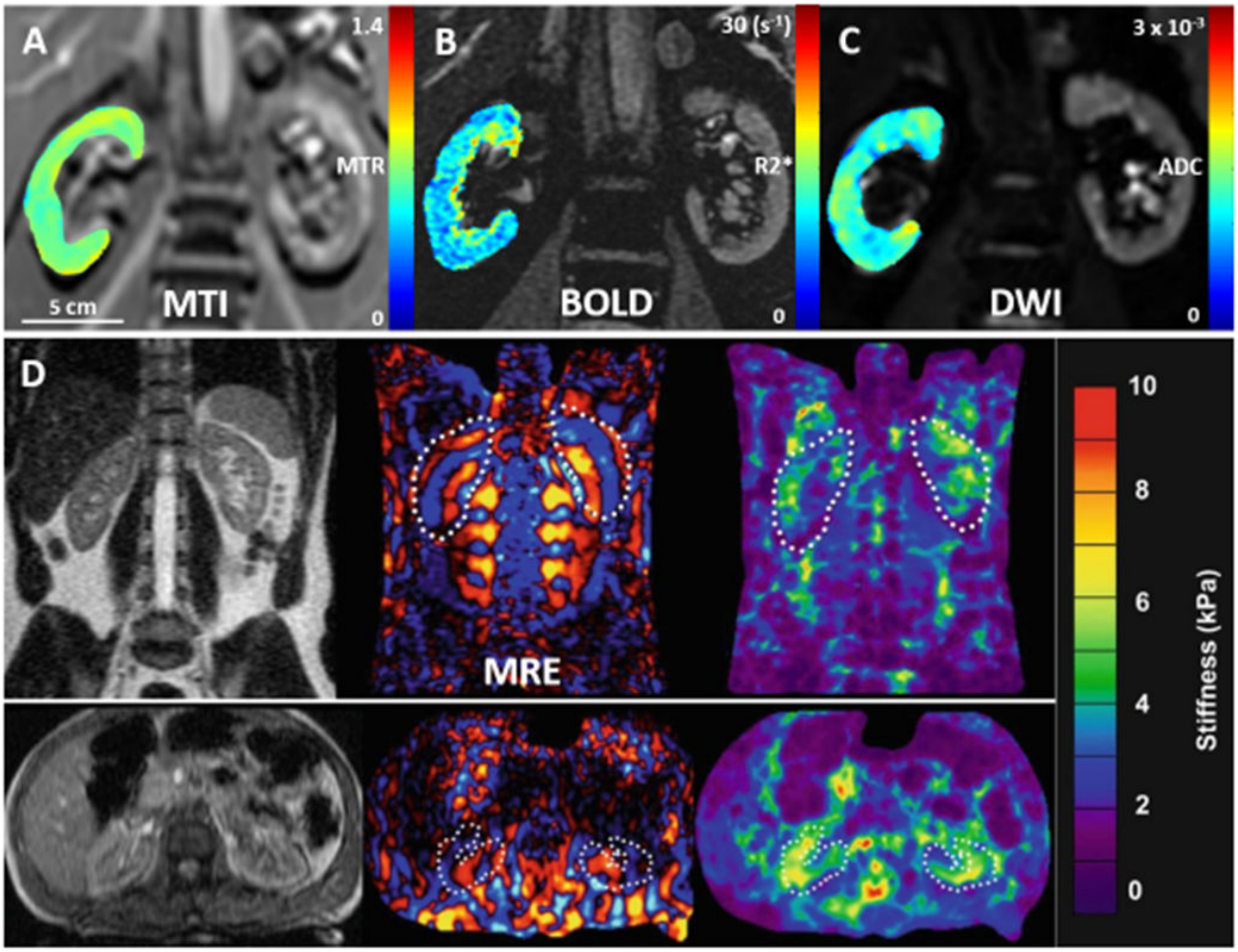

Figure 3. Multi-parametric MRI sequences in the human kidney.

Representative renal MRI maps obtained in the same healthy human subject, depicting: (A) magnetization-transfer ratio (MTR) via magnetization transfer imaging (MTI), which provides an index of fibrosis (green to light yellow is normal; darker yellow to red indicates fibrosis); (B) blood-oxygen level-dependent (BOLD)-MRI R2* parametric map, a reflection of renal oxygenation (blue to light yellow is normal; orange-red indicates renal hypoxia); and (C), an apparent diffusion coefficient (ADC) map obtained by diffusion-weighted imaging (DWI), used to detect changes in renal microstructure and obstruction to water molecule motion (green to light yellow is normal; dark blue indicate lower diffusion and, potentially, fibrosis). This healthy human kidney does not exhibit significant fibrosis. (D) Representative MR elastography (MRE) images of the kidneys acquired in two healthy volunteers, in coronal and axial plane. Middle panels show wave images, while right panels show stiffness maps. Panel D was reprinted from Serai SD, Yin M. MR Elastography of the Abdomen: Basic Concepts. Methods Mol Biol. 2021; 2216:301-323 [64], under the terms of Creative Commons Attribution 4.0 (CC-BY-4.0) International license.

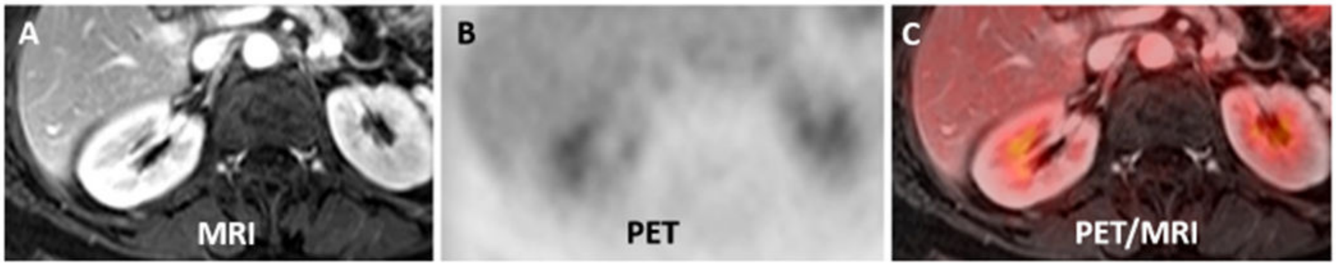

Figure 4. Hybrid imaging of the human kidney.

Representative images depicting A) axial contrast-enhanced volumetric interpolated breath-hold examination, B) axial 18 F-fluorodeoxyglucose PET, and C) fused PET/MRI of the kidneys. Co-registration and fusion of PET and MRI uniquely combines high anatomical detail with functional and molecular information. Adapted by permission from Springer Nature Customer Service Centre GmbH: Suarez-Weiss KE, Herold A, Gervais D, et al. Hybrid imaging of the abdomen and pelvis. Der Radiologe. 2020; 60(Suppl 1):80-89 [88].

Table 1.

Overview of potential applications of different imaging techniques currently available or potentially relevant for clinical kidney imaging. The most promising ones are highlighted in bold.

	US	MRI	CT	PET	Scintigraphy
Renal structure and morphology					
Renal size	✓	✓	✓		
Renal roughness			✓		
Adiposity	✓	✓	✓		
Kidney stones	✓		✓		
Renal artery evaluation	✓	✓ (MRA)	✓		
Perfusion	✓ **(CEUS, SMI, 3D-US)**	✓ (PC, **ASL**, USPIO)	✓ (CE-CT)	✓	✓ (99mTc DTPA, 99mTc MAG3, 99mTc PAH)
Function and metabolism					
GFR		✓ (DCE)	✓ (CE-CT)		✓ (99mTc DTPA, 99mTc PAH)
Tubular function		✓ (**BOLD**)			✓ (99mTc MAG3)
Solute transport		✓ (**23-Na**, K)			
Metabolism		✓ (HP-13C)		✓ (FDG)	
Oxygenation					
Oxygen consumption		✓ (**BOLD**)			
Ischemia		✓ (**DWI**, HP-13C, CEST)			
Viability		✓ (ME)			
Microstructure					
Fibrosis	✓ (B-mode, UE, **CEUS**)	✓ (**DWI**, MRE, MRR, **MTI**, mMRI)	✓		✓ (99mTc DMSA)
Microstructure	✓ (**CEUS**)	✓ (**DWI, DTI,** MRR)			
Stiffness	✓ (UE)	✓ (MRE)			
Interstitium					
Inflammation and edema	✓ (**CEUS**)	✓ (MRR, SPIO)		✓ (CXCR4)	✓ (99mTc OKT3)
Abscess/infection	✓	✓	✓	✓ (FDG)	

Abbreviations: ASL=arterial spin labelling, BOLD=blood oxygenation level dependent, CEST=chemical exchange saturation transfer, CEUS=contrast-enhanced ultrasound, CT=computed-tomography, CXCR4=chemokine receptor-4, DCE=dynamic contrast-enhanced, DMSA=dimercaptosuccinic acid, DTPA= diethylenetriaminepentaacetic acid, DWI=diffusion-weighted imaging, FDG=fluoro-deoxy-glucose, HP-13C=hyperpolarised carbon-13, K=potassium, MAG3= mercaptoacetyltriglycine, ME=dynamic manganese-enhanced, mMRI=molecular MRI, MRA=magnetic resonance angiography, MRE=magnetic resonance elastography, MRI=magnetic resonance imaging, MRR=magnetic resonance relaxometry, MTI = magnetization transfer imaging, PAH= p-aminohippuric acid, PC=phase-contrast, PET=positron emission tomography, SMI=superb microvascular imaging, SPIO=superparamagnetic iron-oxide enhanced, Tc=Technetium, UE=ultrasound elastography, US=ultrasound, USPIO = ultra-small superparamagnetic iron-oxide.

Table 2.

Limitations and advantages of available renal imaging techniques

	US	MRI	CT	PET	Scintigraphy
Availability	++++	++	+++	+	+++
Radiation exposure	no	no	++	++++	++++
Contrast agent	Gas-filled microbubbles for CEUS only (allows only vascular imaging, due to the microbubbles size). Very rare complement activation-related pseudoallergy	Gd-based contrast media for few sequences only (DCE, mMRI). Very rare allergic reactions. Risk of NSF, older generation agents contraindicated in patients with GFR<30. Gd retention in the brain	Iodinated contrast media for most indications. Rare allergic reaction. Few side-effects. Risk of contrast-induced nephropathy (GFR<60)	Radiopharmaceutical needed (mainly FDG). No known side effects	Radiopharmaceutical needed (mainly 99mTc DTPA, DMSA or MAG3). Rare and usually mild allergic reaction
Radiotracers	no	no	no	++++	++++
Cost	+	+++	++	++++	+++
Acquisition time	++	+++	+	++++	++++
Spatial resolution	+ (US), +++ (CEUS, SMI)	+++	++++	++	++
Temporal resolution	+++ (CEUS)	++ (DCE)	++++	+	+
3D	no	yes	yes	yes	no
Versatility	+++	++++	no	+	+
Clinical contraindications	None	Metal implants or devices (cardiac pacemakers and implantable cardioverter defibrillators, neurostimulators, ferromagnetic brain aneurysm clips), presence of foreign bodies, claustrophobia	Pregnancy, Hyperthyroidism (CE-CT), claustrophobia	Pregnancy claustrophobia	Pregnancy claustrophobia
Patient weight limit	no	++++	+++	+++	+++
Operator-dependence	++++	++	+	+	+
Patient comfort	++++	++	++	+	+

Abbreviations: CE-CT=contrast-enhanced CT, CEUS=contrast-enhanced ultrasound, CT=computed tomography, DCE=dynamic contrast-enhanced, DMSA= dimercaptosuccinic acid, DTPA= diethylenetriaminepentaacetic acid, Gd=Gadolinium, GFR=glomerular filtration rate, MAG3= mercaptoacetyltriglycine, MRI=magnetic resonance imaging, mMRI=molecular MRI, NSF=nephrogenic systemic fibrosis, PET=positron-emission tomography, SMI=superb microvascular imaging, Tc=Technetium, US=ultrasound.